A Letters Journal Exploring the Frontiers of Physics

January 2008

EPL, **81** (2008) 27003 www.epljournal.org
doi: 10.1209/0295-5075/81/27003

Large optical gain from four-wave mixing instabilities in semiconductor quantum wells

S. Schumacher, N. H. Kwong and R. Binder

College of Optical Sciences, University of Arizona - Tucson, AZ 85721, USA

received 13 August 2007; accepted in final form 9 November 2007
published online 6 December 2007

PACS 71.35.-y – Excitons and related phenomena
PACS 78.47.+p – Time-resolved optical spectroscopies and other ultrafast optical measurements in condensed matter
PACS 42.65.Sf – Dynamics of nonlinear optical systems; optical instabilities, optical chaos and complexity, and optical spatio-temporal dynamics

Abstract – Based on a microscopic many-particle theory, we predict large optical gain in the probe and background-free four-wave mixing directions caused by excitonic instabilities in semiconductor quantum wells. For a single quantum well with radiative-decay limited dephasing in a typical pump-probe setup we discuss the microscopic driving mechanisms and polarization and frequency dependence of these instabilities.

In gaseous atomic or molecular systems and simple Kerr media, four-wave mixing (FWM) processes lead, among other things, to transverse optical instabilities (*e.g.*, refs. [1–5]). The interest in these FWM instabilities has recently been renewed by the demonstration of their effectiveness for all-optical switching at very low light intensities [6,7]. In this letter we argue on the basis of a microscopic many-particle analysis that FWM instabilities can occur via nonlinear excitonic processes in a single semiconductor quantum well (QW). Instead of studying spontaneous off-axis pattern formation induced by these instabilities, we investigate their role in a pump-probe setup as illustrated in fig. 1. We find that the FWM instabilities can lead to large gain in the probe and (background-free) FWM directions that grows exponentially with the pump pulse duration, limited by the eventual buildup of incoherent exciton/biexciton densities. Our analysis shows that the materials conditions for observing these instability-induced gains, though quite stringent, appear to be obtainable in currently available high-quality QW samples.

FWM has been widely used in studies of microscopic processes in QWs (*e.g.*, refs. [8–15]). An example of FWM-driven instabilities in semiconductors is the parametric amplification of exciton polaritons in planar QW microcavities [16–23]. In contrast to the microcavity, we focus on the "simple" system of a single QW. Using a microscopic many-particle theory we give a comprehensive stability analysis of the optical polarization field

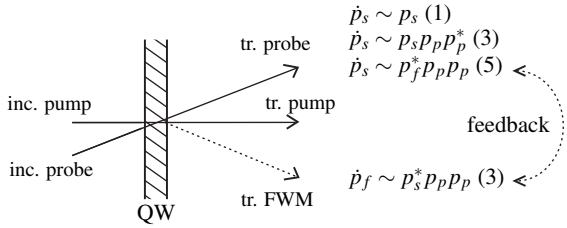

Fig. 1: Illustration of the investigated pump-probe setup, including incoming and transmitted light pulses (reflected pulses are omitted for clarity) for probe, pump, and FWM direction (the angle between the different propagation directions is strongly exaggerated). Selected contributions to the probe and FWM polarizations are schematically included in the figure. The numbers in parentheses indicate the lowest order in the external fields in which they appear.

induced by a normally incident pump beam, treating all vectorial polarization state channels. In atomic systems, phase-space filling (PSF) nonlinearities drive the instabilities, and in microcavities it is the interaction between co-circularly (say, ++) polarized polaritons, related to the Hartree-Fock (HF) interaction and two-exciton (++) correlations [21–23]. We find that neither PSF nor excitonic interactions in the ++ channel are promising for instabilities in single QWs, mainly because of excessive excitation-induced dephasing (EID). Instead we show that instabilities and large probe gains can be produced in single QWs by virtual biexciton formation, which requires

$$
\begin{aligned}
i\hbar\dot{p}^{\pm}_{s,f} &= (\varepsilon_x - i\gamma)p^{\pm}_{s,f} - \left[\phi^*_{1s}(0) - 2A^{\mathrm{PSF}}|p^{\pm}_p|^2\right]d_{cv}E^{\pm}_{s,f} + 2d_{cv}A^{\mathrm{PSF}}\left[p^{\pm}_{s,f}p^{\pm *}_p E^{\pm}_p + p^{\pm *}_{f,s}p^{\pm}_p E^{\pm}_p\right] \\
&+2V^{\mathrm{HF}}|p^{\pm}_p|^2 p^{\pm}_{s,f} + 4p^{\pm *}_p \int_{-\infty}^{\infty} \mathrm{d}\,t' \mathcal{G}^{\pm\pm}(t-t')p^{\pm}_p(t')p^{\pm}_{s,f}(t') + V^{\mathrm{HF}}p^{\pm 2}_p p^{\pm *}_{f,s} + 2p^{\pm *}_{f,s}\int_{-\infty}^{\infty} \mathrm{d}\,t' \mathcal{G}^{\pm\pm}(t-t')p^{\pm}_p(t')p^{\pm}_p(t') \\
&+p^{\mp *}_p \int_{-\infty}^{\infty} \mathrm{d}\,t' \mathcal{G}^{\pm\mp}(t-t')\left[p^{\mp}_p(t')p^{\pm}_{s,f}(t') + p^{\pm}_p(t')p^{\mp}_{s,f}(t')\right] + p^{\mp *}_{f,s}\int_{-\infty}^{\infty} \mathrm{d}\,t' \mathcal{G}^{\pm\mp}(t-t')p^{\pm}_p(t')p^{\mp}_p(t')\,. \qquad (1)
\end{aligned}
$$

the pump to contain both circular polarizations (*e.g.*, to be linearly polarized). Biexciton-induced bistabilities and instabilities have been studied before, but in bulk semiconductors (*e.g.*, for CuCl [24–27]), rather than in quasi–two-dimensional QWs studied here. These early works used bosonic models and did not consider optical gain in the off-pump directions. It has been established (*e.g.*, refs. [28–30]) that for typical QW systems (*e.g.*, GaAs, ZnSe) a fermionic microscopic theory, as used in this paper, is needed for the understanding of excitonic PSF, spin-dependent exciton interactions giving rise to excitonic HF mean-field effects, as well as retarded exciton interactions that can result in the bound two-exciton state (biexciton) and two-exciton continuum states, EID, and quantum memory effects.

We investigate a pump-probe setup as illustrated in fig. 1 with the light propagating in quasi-normal incidence and with all optical pulses spectrally centered near the $1s$ heavy-hole (hh) exciton resonance. Assuming all other resonances to be sufficiently far away, the coherent response of the system in the lowest-order nonlinear regime ($\chi^{(3)}$-regime) has been well studied. We focus our analysis on small pump intensities where the many-particle effects listed above are dominant for the coherent optical QW response (*i.e.*, we neglect higher than four-fermion or two-exciton correlations). The influence of higher-order correlations and incoherent exciton contributions is discussed later in our analysis. We start from the nonlinear equation for the optically induced interband polarization $p^{\pm}$ ($+,-$ label the circular polarization states) and perform a spatial Fourier decomposition of $p^{\pm}$ and the exciting field $E^{\pm}$ with respect to the in-plane wave vector k. We label the Fourier components with the subscripts s, f and p for probe (also called signal, with $k = k_s$, assumed to be small but nonzero), background-free FWM ($k = -k_s$), and pump ($k = 0$) direction, respectively. The resulting equations are linearized in the weak probe field $E^{\pm}_s$ but solved self-consistently in the pump field $E^{\pm}_p$ [31,32]. The equations for $p^{\pm}_{s,f}$ read:

see eq. (1) *above*

The nonlinear pump equation for $p^{\pm}_p$ (not shown) involves the same nonlinear processes. We note that the solution to eq. (1) goes beyond the $\chi^{(3)}$-limit and includes the pump polarization up to arbitrary order. Here, ε_x is the $1s$-hh exciton energy, γ a phenomenological excitonic dephasing constant (not including the radiative decay),

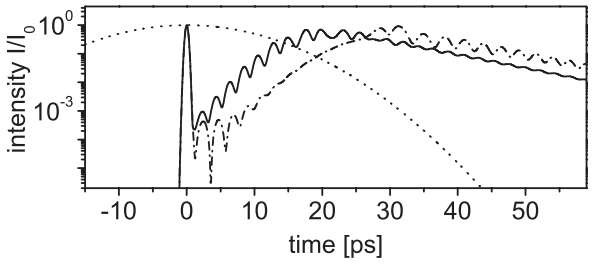

Fig. 2: Transmitted intensity of a 500 fs probe (normalized to the peak intensity I_0 of the incoming probe). The shape of the 20 ps pump pulse is included as a dotted line. Results are shown for XX pump-probe polarization, zero pump-probe delay, pump peak intensities $22\,\mathrm{kW\,cm^{-2}}$ (solid line) and $5.3\,\mathrm{kW\,cm^{-2}}$ (dash-dotted line), and equal pump and probe central frequencies tuned to -0.6 meV (solid line) and -1.2 meV (dash-dotted line) below the exciton resonance, respectively.

d_{cv} the interband dipole matrix element, $\phi_{1s}(\mathbf{r})$ the two-dimensional exciton wave function, A^{PSF} the excitonic PSF constant, and V^{HF} the excitonic HF matrix element. Unless otherwise noted, the time argument is t. The correlation kernels $\mathcal{G}$ are given by $\mathcal{G}^{++} = \mathcal{G}^{--} = \tilde{G}^{+}$ and $\mathcal{G}^{+-} = \mathcal{G}^{-+} = \tilde{G}^{+} + \tilde{G}^{-}$, with $\tilde{G}^{\pm}$ as defined in eq. (22) in ref. [30], including a two-exciton dephasing rate 2γ. The propagation of the optical field $E^{\pm}$ across the QW is described with a transfer-matrix method accounting for radiative corrections/decay and assuming the QW to be infinitely thin (*e.g.*, ref. [33]).

From a time-domain solution[1] of eq. (1) and the equation for the nonlinear pump polarization, we find for the co-linear (XX) pump-probe polarization configuration for certain pump detunings $\Delta\varepsilon = \hbar\omega_p - \varepsilon_x$ and above a certain pump threshold intensity I_{th} a large energy transfer from the pump into the probe and FWM directions. To illustrate this phenomenon, fig. 2 shows the transmitted probe intensity for two different $\Delta\varepsilon$ which —after the initial probe has passed— grows (almost) exponentially until the pump-induced QW polarization (not shown) falls below a certain threshold value (calculations for a high-quality GaAs QW at low temperatures where the radiative decay dominates the homogeneous linewidth as, *e.g.*, in ref. [15]). For the results in fig. 2 about two orders of magnitude

[1] Parameters: $\varepsilon_x = 1.4965\,\mathrm{eV}$, $E^{xx}_b \approx 1.84\,\mathrm{meV}$, $d_{cv} = 4\,e\text{Å}$, $\gamma = 0.01\,\mathrm{meV}$, $A^{\mathrm{PSF}} = 4a^x_0\sqrt{2\pi}/7$, $V^{\mathrm{HF}} = 2\pi(1 - 315\pi^2/4096)a^{x2}_0 E^x_b$, with $a^x_0 \approx 170\,\text{Å}$, $E^x_b \approx 13\,\mathrm{meV}$.

of time-integrated gain in the probe direction are found. We find similar outgoing fluences in the background-free FWM directions (not shown).

To analyze the gain mechanism, we supplement the full time-dependent solution by a linear stability analysis (LSA). The LSA is done without an incoming probe field and for a monochromatic cw pump field $E_p^{\pm}(t) = \tilde{E}_p^{\pm} \mathrm{e}^{-i\omega_p t}$ and pump polarization $p_p^{\pm}(t) = \tilde{p}_p^{\pm} \mathrm{e}^{-i\omega_p t}$, with $\dot{\tilde{p}}_p^{\pm} = \dot{\tilde{E}}_p^{\pm} = 0$ (ω_p is the pump frequency). We evaluate the memory integrals in eq. (1) in Markov approximation $[p_{s,f}(t') \approx p_{s,f}(t)\mathrm{e}^{i\omega_p(t-t')}]$ for the two-exciton continuum in the correlation kernels $\mathcal{G}^{\pm\pm}$, $\mathcal{G}^{\pm\mp}$. In contrast, exact treatment of the bound biexciton state (included in the correlation kernel $\mathcal{G}^{\pm\mp}$ in eq. (1) [30]) via the time-dependent amplitudes $b_{s,f}(t)$ is crucial to include the related quantum memory effects (*e.g.*, refs. [34–36]) which —as our analysis reveals— give rise to additional unstable modes. According to eq. (1) the term driving the bound biexciton amplitudes $b_{s,f}(t)$ is proportional to $p_p^{\mp} p_{s,f}^{\pm} + p_p^{\pm} p_{s,f}^{\mp}$. With the ansatz $p_{s,f}(t) = \tilde{p}_{s,f}(t)\mathrm{e}^{-i\omega_p t}$ and $b_{s,f}(t) = \tilde{b}_{s,f}(t)\mathrm{e}^{-i2\omega_p t}$ the probe and FWM dynamics take the form $\frac{\mathrm{d}}{\mathrm{d}t}\tilde{\mathbf{p}}(t) = M\,\tilde{\mathbf{p}}(t)$, with $\tilde{\mathbf{p}}(t) = \left[\tilde{p}_s^{+}(t), \tilde{p}_f^{+*}(t), \tilde{p}_s^{-}(t), \tilde{p}_f^{-*}(t), \tilde{b}_s(t), \tilde{b}_f^{*}(t)\right]^T$ where the matrix M follows from eq. (1). If at least one of the eigenvalues λ_i of M fulfills $\mathrm{Re}\{\lambda_i\} > 0$, the system is unstable. An arbitrarily small seed of $p_{s,f}^{\pm}$ would grow exponentially, until the matrix M ceases to describe the system correctly.

On the PSF level (only line 1 of eq. (1)) the nonlinear terms from left to right are: i) nongrating Pauli-blocking, ii) self-wave mixing (SWM) including power broadening with the general structure $i\dot{p}_{s,f} \sim p_{s,f} p_p^* E_p$, and iii) the phase-conjugate oscillation (PCO) with the structure $i\dot{p}_{s,f} \sim p_{f,s}^* p_p E_p$ which gives the feedback between probe and FWM signal (compare fig. 1) which drives the instability in atomic systems, *e.g.*, in ref. [1]. Going beyond the PSF level, in the second line of eq. (1), HF exciton Coulomb interaction and excitonic correlations (the two-exciton continuum in the electron-spin triplet (++) channel) contribute to the two-exciton interaction. While the first two of these terms are of the SWM type ($i\dot{p}_{s,f} \sim p_{s,f} p_p^* p_p$) and basically blue-shift the exciton resonance in eq. (1) and lead to additional EID, the last two terms have the general structure of a PCO contribution ($i\dot{p}_{s,f} \sim p_{f,s}^* p_p p_p$) mediated by the two-exciton Coulomb interaction. The third line in eq. (1) contains the Coulomb interaction in the two-exciton electron-spin singlet (+−) channel, including both the bound biexciton state and the two-exciton continuum in this channel, where the first term is of the SWM type and the last term has the structure of a PCO coupling.

We start the discussion with a σ^+ polarized pump. Without Coulomb interaction, only the PSF-PCO can lead to an instability as it is the case in atomic systems. However, within our model with zero in-plane exciton polariton dispersion, one can show analytically that PSF alone does not yield an instability (*i.e.*, all $\mathrm{Re}\{\lambda_i\} < 0$), which is analogous to the forward propagating case in atomic systems [2]; PSF-SWM and PSF-PCO counteract each other. We note that an extension of eq. (1) to realistic nearly quadratic dispersions [37] [$\varepsilon_x \equiv \varepsilon_x(k)$] can —in principle— yield instabilities for certain positive pump detuning $\varepsilon_x(0) < \hbar\omega_p < \varepsilon_x(k_s)$, however, our numerical studies have shown that they occur only at extremely high intensities, rendering the instabilities unlikely to be experimentally observable and justifying the neglect of the in-plane dispersion.

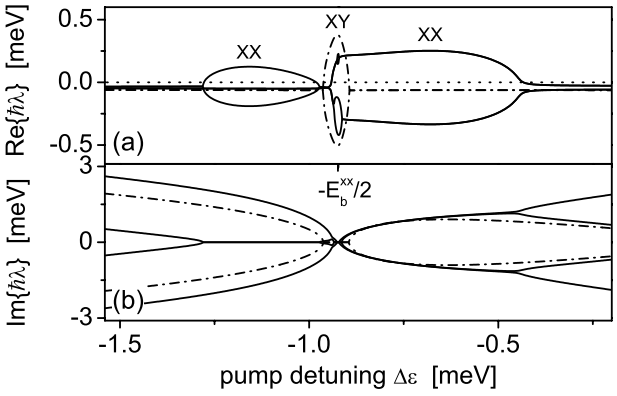

Fig. 3: Linear stability analysis for a linearly polarized pump for steady-state total coherent exciton density $n_x^{\mathrm{total}} = 1.6 \times 10^{10}\,\mathrm{cm}^{-2}$. Shown are the real parts (a) and imaginary parts (b) of the eigenvalues λ_i of the matrix M for negative pump detuning. Eigenvalues are represented by solid lines for the co-linear (XX) and by dash-dotted lines for the cross-linear (XY) polarization configuration. The corresponding pump intensity and exciton ($|p_p^{\mathrm{X}}|^2$) and biexciton ($2|b_p|^2$) contributions to n_x^{total} are depicted in fig. 4. The dotted line in panel (a) separates the stable ($\mathrm{Re}\{\lambda\} < 0$) from the unstable ($\mathrm{Re}\{\lambda\} > 0$) regime.

Without in-plane dispersion and including only HF terms (which, physically, leads to an exciton blue-shift caused by the HF-SWM terms), we found from a numerical diagonalization of M, instabilities in a small spectral window for positive pump detuning, mediated by the HF-PCO contribution. In planar semiconductor microcavities, the parametric polariton amplification has been attributed to this instability [16–22]. However, two-exciton correlations in the electron-spin triplet (++) channel [30] have been found to weaken this instability [23], and in our case of a single QW we find that for realistic parameters the instability is inhibited when these correlations are taken into account; mainly because of EID due to two-exciton scattering.

In contrast, a regime where excitonic correlations are strong but EID is kept small can be accessed for negative pump detuning $\Delta\varepsilon < 0$ with a linearly (say X) polarized pump that also excites the excitonic correlations in the electron-spin singlet (+−) channel. The corresponding eigenvalues of M are shown in fig. 3 for a fixed total coherent exciton density defined as $n_x^{\mathrm{total}} \equiv |p_p^{\mathrm{X}}|^2 + 2|b_p|^2$

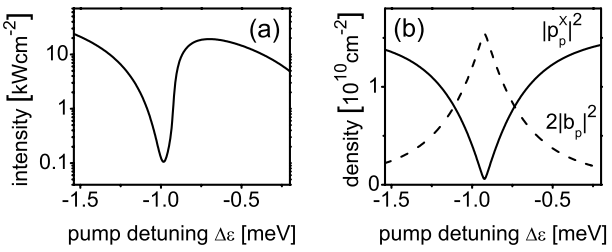

Fig. 4: (a) Pump intensity corresponding to the total coherent exciton density $n_x^{\rm total} = 1.6 \times 10^{10}\,{\rm cm}^{-2}$ used in fig. 3. (b) Exciton ($|p_p^{\rm X}|^2$) and biexciton ($2|b_p|^2$) contributions to $n_x^{\rm total}$.

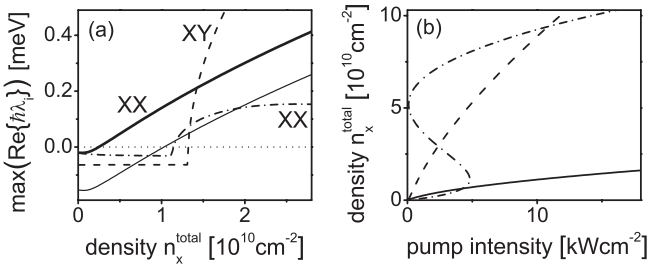

Fig. 5: (a) Real part of the eigenvalue λ_i of M with the largest real part corresponding to co-linear (XX) and cross-linear (XY) pump-probe polarization configuration, respectively. (b) Total coherent exciton density $n_x^{\rm total}$ *vs.* pump intensity inside the QW. (a), (b) Results are shown for different pump detunings, $\Delta\varepsilon = -0.6\,{\rm meV}$ (solid line), $\Delta\varepsilon = -0.92\,{\rm meV}$ (dashed line), and $\Delta\varepsilon = -1.2\,{\rm meV}$ (dash-dotted line). The thin solid line in (a) shows the same result as the thick solid line but for a ten times larger dephasing $\gamma = 0.1\,{\rm meV}$.

with the coherent exciton ($|p_p^{\rm X}|^2$) and bound biexciton ($|b_p|^2$) densities (for $\Delta\varepsilon < 0$ we have checked that density contributions from the two-exciton continuum are negligible compared to $n_x^{\rm total}$). The pump polarization $p_p^{\rm X}$ induced by the X polarized pump follows from the (cubic) nonlinear pump equation and b_p is the bound biexciton amplitude driven by a source term proportional to $p_p^+ p_p^-$. The pump intensity and exciton and biexciton contributions to $n_x^{\rm total}$ are depicted in fig. 4.

In fig. 3(a) we find three different unstable regions ($\mathrm{Re}\{\lambda\} > 0$) caused by the biexcitonic ($+-$) PCO terms in eq. (1). The labels XX and XY denote the vectorial polarizations of the pump (always X) and the unstable modes or probe fluctuations (either X or Y). The dependence of the eigenvalues with the largest real parts (which, when positive, are the maximum growth rates) on $n_x^{\rm total}$ is shown in fig. 5(a) (with fig. 5(b) relating $n_x^{\rm total}$ to the pump intensity). Clearly, the LSA helps us understand the temporal growth in fig. 2, with maximum coherent densities $n_x^{\rm total} \approx 1.8 \times 10^{10}\,{\rm cm}^{-2}$ ($22\,{\rm kW\,cm}^{-2}$) and $\approx 3.5 \times 10^{10}\,{\rm cm}^{-2}$ ($5.3\,{\rm kW\,cm}^{-2}$).

We consider a range of relatively small total coherent densities $n_x^{\rm total} \lesssim 3 \times 10^{10}\,{\rm cm}^{-2}$ to minimize the influence of higher-order correlations not included in our theory. This restriction limits the maximum growth rates in the unstable regime (fig. 5(a)) and therefore dictates the minimum timescale that is required to achieve a desired amount of gain. In principle, accumulation of an incoherent exciton/biexciton density in the system on this timescale (leading to additional EID) can cap the possible amount of gain. However, for the timescales in fig. 2 we believe that additional EID from incoherent densities would not crucially affect the presented results[2]. In addition to the EID from incoherent densities, the exponential growth of gain with increasing pump length can also be limited by depletion of the pump signal, if, after a certain growth period, the probe and FWM signals have become sufficiently strong so that linearization of the polarization dynamics in these signals is no longer valid. Finally, in fig. 5(a) we show how the instability threshold density changes by increasing the effective dephasing in the system (*e.g.*, by increasing temperature or due to EID). As a relatively sharp spectral feature around the two-photon biexciton resonance (fig. 3(a)) the XY instability may not be robust against even small deviations from the model conditions considered here. Therefore, in the following, we focus our attention on the unstable modes in the XX configuration.

We can distinguish i) an XX instability below ($\Delta\varepsilon < -E_b^{xx}/2$) and ii) above ($\Delta\varepsilon > -E_b^{xx}/2$) the two-photon biexciton resonance at $\Delta\varepsilon = -E_b^{xx}/2 \approx -0.92\,{\rm meV}$. Focusing on i), we see from fig. 5(b) that it occurs in a region of bistability (*i.e.*, three possible steady-state coherent exciton densities for fixed intensity). In the corresponding time domain calculation in fig. 2 the instability of the intermediate branch of the bistable pump solution (cf. ref. [27]) is reflected in the exponentially growing probe signal over time, and as demonstrated in fig. 2 can give rise to large probe gain. However, we note that in this bistable regime the system dynamics sensitively depends on the "initial conditions", determined by the overall temporal pump pulse shape. In fig. 2 we use a Gaussian pump pulse with intensity and pulse length chosen such that the pulse induces a coherent density on the intermediate (unstable) branch in the bistable regime (cf. dash-dotted line in fig. 5(b)). However, for a different choice of pump parameters the induced polarization may have mainly contributions from the lower and upper (stable) branches, so that no exponential growth (instability) in fig. 2 would be observed. Turning to the instability ii), we find a much lower threshold (as low as $n_x^{\rm total} \approx 3 \times 10^9\,{\rm cm}^{-2}$) than for the other configurations. Furthermore, fig. 3(b) explains

[2]For pump excitation below the exciton resonance, energy conservation dictates that only scatterings from coherent and incoherent bound biexcitons (the incoherent biexciton density does not exceed $\approx 2.5 \times 10^9\,{\rm cm}^{-2}$ for the results shown in fig. 2) can efficiently cause EID losses for the coherent exciton and biexciton densities. Assuming that the scattering rates for processes involving at least one bound biexciton are considerably lower than for two-exciton scattering, these EID contributions are negligible for the timescales considered in this paper.

the apparent beating on the probe signal (solid line in fig. 2) during the exponential growth period. In case ii), the unstable modes exist in pairs with complex conjugate eigenvalues. Whereas the growth rates, $\mathrm{Re}\{\lambda\}$, are the same for the two modes in each pair, the frequencies, $\mathrm{Im}\{\lambda\}$, have opposite signs. The unstable growth of the probe and FWM signals occurs at the two frequencies $\omega_p \pm |\mathrm{Im}\{\lambda\}|$. This is inherently related to a non-Markovian quantum memory effect, brought about by the time-retarded structure of the biexcitonic SWM term in eq. (1).

Our analysis is applicable to other semiconductor materials provided suitable scalings in lengths (with a_0^x) and energies (with E_b^x) are made. Since we believe that FWM instabilities in QWs can be expected as long as the excitonic dephasing is not much larger than the radiative decay (*e.g.*, $\approx 0.05\,\mathrm{meV}$ for GaAs [15], $\approx 0.3\,\mathrm{meV}$ for ZnSe), materials with a very small ratio γ/E_b^x would be ideal.

In conclusion, we predict optical FWM instabilities and corresponding strong probe and FWM signal gain in a semiconductor QW. Further research, *e.g.*, into possible transverse pattern formation and propagation effects in multiple QWs, would be desirable.

* * *

We thank A. L. Smirl, University of Iowa, for generously sharing his ideas and insights on the subject matter with us. This work has been supported by ONR, DARPA, and JSOP. S. Schumacher gratefully acknowledges support by the Deutsche Forschungsgemeinschaft (SCHU 1980/3-1).

REFERENCES

[1] Yariv A. and Pepper D. M., *Opt. Lett.*, **1** (1977) 16.
[2] Grynberg G., *Opt. Commun.*, **66** (1988) 321.
[3] Chang R., Firth W. J., Indik R., Moloney J. V. and Wright E. M., *Opt. Commun.*, **88** (1992) 167.
[4] Honda T., *Opt. Lett.*, **18** (1993) 598.
[5] Firth W. J., Fitzgerald A. and Par C., *J. Opt. Soc. Am. B*, **7** (1990) 1087.
[6] Dawes A. M. C., Illing L., Clark S. M. and Gauthier D. J., *Science*, **308** (2005) 672.
[7] Chen Y. F., Tsai Z. H., Liu Y. C. and Yu I. A., *Opt. Lett.*, **30** (2005) 3207.
[8] Leo K., Wegener M., Shah J., Chemla D. S., Göbel E. O., Damen T. C., Schmitt-Rink S. and Schäfer W., *Phys. Rev. Lett.*, **65** (1990) 1340.
[9] Paul A. E., Bolger J. A., Smirl A. L. and Pellegrino J. G., *J. Opt. Soc. Am. B*, **13** (1996) 1016.
[10] Bartels G., Stahl A., Axt V., Haase B., Neukrich U. and Gutowski J., *Phys. Rev. Lett.*, **81** (1998) 5880.
[11] Wang H., Hou H. Q. and Hammons B. E., *Phys. Rev. Lett.*, **81** (1998) 3255.
[12] Cundiff S. T., *Phys. Rev. A*, **49** (1994) 3114.
[13] Banyai L., Thoai D. B. T., Reitsamer E., Haug H., Steinbach D., Wehner M. U., Wegener M., Marschner T. and Stolz W., *Phys. Rev. Lett.*, **75** (1995) 2188.
[14] Bolton S. R., Neukirch U., Sham L. J., Chemla D. S. and Axt V. M., *Phys. Rev. Lett.*, **85** (2000) 2000.
[15] Langbein W., Meier T., Koch S. W. and Hvam J. M., *J. Opt. Soc. Am. B*, **18** (2001) 1318.
[16] Savvidis P. G., Baumberg J. J., Stevenson R. M., Skolnick M. S., Whittaker D. M. and Roberts J. S., *Phys. Rev. Lett.*, **84** (2000) 1547.
[17] Stevenson R. M., Astratov V. N., Skolnick M. S., Whittaker D. M., Eman-Ismail M., Tartakovskii A. I., Savvidis P. G., Baumberg J. J. and Roberts J. S., *Phys. Rev. Lett.*, **85** (2000) 3680.
[18] Saba M., Ciuti C., Bloch J., Thierry-Mieg V., Andre R., Le Si Dang, Kundermann S., Mura A., Bongiovanni G., Staehli J. L. and Deveaud B., *Nature*, **414** (2001) 731.
[19] Gippius N. A., Tikhodeev S. G., Kulakovskii V. D., Krizhanovskii D. N. and Tartakovskii A. I., *Europhys. Lett.*, **67** (2004) 997.
[20] Diederichs C., Tignon J., Dasbach G., Ciuti C., Lemaitre A., Bloch J., Roussignol P. and Delalande D., *Nature*, **440** (2006) 904.
[21] Ciuti C., Schwendimann P. and Quattropani A., *Semicond. Sci. Technol.*, **18** (2003) 279.
[22] Whittaker D. M., *Phys. Rev. B*, **71** (2005) 115301.
[23] Savasta S., Di Stefano O. and Girlanda R., *Phys. Rev. Lett.*, **90** (2003) 096403.
[24] Inoue M., *Phys. Rev. B*, **33** (1986) 1317.
[25] Koch S. W. and Haug H., *Phys. Rev. Lett.*, **46** (1981) 450.
[26] Peyghambarian N., Gibbs H. M., Rushford M. C. and Weinberger D. A., *Phys. Rev. Lett.*, **51** (1983) 1692.
[27] Nguyen D. T., *Phys. Lett. A*, **193** (1994) 462.
[28] Axt V. M. and Stahl A., *Z. Phys. B*, **93** (1994) 195.
[29] Östreich T., Schönhammer K. and Sham L. J., *Phys. Rev. Lett.*, **74** (1995) 4698.
[30] Takayama R., Kwong N. H., Rumyantsev I., Kuwata-Gonokami M. and Binder R., *Eur. Phys. J. B*, **25** (2002) 445.
[31] Buck M., Wischmeier L., Schumacher S., Czycholl G., Jahnke F., Voss T., Rückmann I. and Gutowski J., *Eur. Phys. J. B*, **42** (2004) 175.
[32] Schumacher S., Czycholl G., Jahnke F., Kudyk I., Wischmeier L., Rückmann I., Voss T., Gutowski J., Gust A. and Hommel D., *Phys. Rev. B*, **72** (2005) 081308(R).
[33] Khitrova G., Gibbs H. M., Jahnke F., Kira M. and Koch S. W., *Rev. Mod. Phys.*, **71** (1999) 1591.
[34] Axt V. M., Kuhn T., Haase B., Neukirch U. and Gutowski J., *Phys. Rev. Lett.*, **93** (2004) 127402.
[35] Shahbazyan T. V., Primozich N. and Perakis I. E., *Phys. Rev. B*, **62** (2000) 15925.
[36] Sieh C., Meier T., Jahnke F., Knorr A., Koch S. W., Brick P., Hübner M., Ell C., Prineas J., Khitrova G. and Gibbs H. M., *Phys. Rev. Lett.*, **82** (1999) 3112.
[37] Tassone F., Bassani F. and Andreani L. C., *Nuovo Cimento*, **12** (1990) 1673.